JOURNAL OF THERMOPHYSICS AND HEAT TRANSFER
Vol. 17, No. 4, October–December 2003

Measurement and Modeling of OH, NO, and CO_2 Infrared Radiation at 3400 K

Denis Packan,* Christophe O. Laux,† Richard J. Gessman,* Laurent Pierrot,‡ and Charles H. Kruger§
Stanford University, Stanford, California 94305-3032

The infrared emission spectrum of an air plasma containing small quantities of CO_2 and H_2O was measured and modeled in absolute intensity in the spectral range 2.4–5.6 μm. A 50-kW radio-frequency inductively coupled plasma torch was used to produce the air plasma in local thermodynamic equilibrium. The temperature profile measured by emission spectroscopy peaks at 3400 K. The absolute intensity emission spectrum was measured and compared with numerical simulations obtained with the line-by-line radiation code SPECAIR. Spectroscopic models incorporated into the SPECAIR code include the infrared rovibrational bands of OH, NO, and CO. Absorption of the plasma emission by room-air CO_2 and H_2O in the optical path between the plasma and the detector is taken into account. Plasma emission from CO_2 ($\nu_1 + \nu_3$) and (ν_3) bands is also modeled, using a correlated-k model. Good agreement is obtained between experiment and modeling.

Introduction

MODELS for infrared spectral emission by heated air and absorption by ambient air are important for in-flight and ground-based detection of infrared signatures. A signature detector placed onboard a high velocity vehicle must look through optically transparent spectral regions of the atmosphere and of the hot shock layer located in front of the vehicle. Accurate radiation models are also important for optical diagnostics in order to determine temperatures and concentrations in both equilibrium and nonequilibrium plasmas. The infrared absorption of ambient air is well documented, and spectroscopic parameters are available in databases.[1] The infrared radiation of heated air, on the other hand, has been the object of fewer investigations, and validation of models is rendered difficult by the lack of accurate experimental results, especially for polyatomic molecules such as water and CO_2.

We have made spectral measurements of the absolute infrared emission of an air plasma at about 3400 K. We have also developed a line-by-line model for diatomic molecules and a correlated-k model for CO_2 emission. In this paper we present our measurements and models and then a comparison of the results.

This work represents the second phase of our effort to model and understand the infrared radiation of air plasmas. The first phase[2] focused on infrared air radiation measurement and modeling for an local thermodynamic equilibrium (LTE) air plasma at about 8000 K and led to the development of the radiation code SPECAIR, as an extension of the NASA code NEQAIR.[3] The second phase, presented here, focuses on LTE air plasmas at about 3400 K, where molecular radiation is predominant and atomic line radiation negligible. The measurements allowed us to test spectroscopic models newly implemented in SPECAIR for OH infrared emission and room air (CO_2 and H_2O) absorption. A correlated-k model for CO_2 emission[4] was also tested.

Presented as Paper 99-3605 at the AIAA 30th Plasmadynamics and Lasers Conference, Norfolk, VA, 28 June–1 July 1999; received 1 July 2002; revision received 12 April 2003; accepted for publication 14 April 2003.

*Doctoral Student, Mechanical Engineering Department, Thermosciences Division. Member AIAA.
†Senior Research Scientist, Mechanical Engineering Department, Thermosciences Division. Associate Fellow AIAA.
‡Postdoctoral Fellow, Mechanical Engineering Department, Thermosciences Division. Member AIAA.
§Professor, Vice-Provost, and Dean of Research and Graduate Policy, Mechanical Engineering Department, Thermosciences Division. Member AIAA.

Experiment

Experimental Setup and Conditions

The experiments were conducted with a 50-kW radio-frequency induction plasma torch operating at atmospheric pressure. The plasma torch is comprised of a TAFA model 66 torch-head powered by a LEPEL model T-50-3 RF power supply operating at a frequency of 4 MHz. The torch facility can produce air plasmas in LTE over a wide range of temperatures (2000–8000 K), allowing measurements under reproducible and well-characterized conditions. As shown in Fig. 1, a 60-cm-long, water-cooled test section was mounted on top of the upward-firing torch. The test section, made of brass, cools down the flowing air plasma to the desired temperature of about 3400 K. The exit plume diameter is 1 cm, and the gas velocity is about 400 m/s. All measurements were made 1 cm downstream of the exit of the test section, in a region where the flow is laminar. The air injected into the torch contained ~330 ppm of CO_2 and $\sim 2.25 \times 10^{-3}$ mole fraction of water vapor.

The setup for spectral measurements, shown in Fig. 2, includes a SPEX model 750M $\frac{3}{4}$-m scanning monochromator fitted with a Cincinnati Electronics model SDD-20E1-S1 indium-antimonide cryogenically cooled (liquid N_2) infrared detector with integrated preamplifier. A 300-groove/mm grating blazed at 4.0 μm was used at first order. The dispersion of the grating is approximately 40 Å/mm. The entrance and exit slit widths were 1 and 2.8 mm, respectively.

Spectra were recorded in the range 2.4–5.6 μm to capture NO fundamental and first overtone, OH fundamental rovibrational bands, and CO_2 bands. To reject second- and higher-order spectra, the spectral acquisition was split into two ranges, 2.4–3.0 and 3.0–5.6 μm, and two long-pass filters with cutoffs at 1.5 and 3.0 μm, respectively, were used.

Emission from the light sources used in this work (plasma or calibration lamp) travels through 6 m of room air before reaching the detector. Emission spectra are therefore affected by absorption from room-air CO_2 and H_2O, which can be significant in the infrared. To model this absorption, the temperature and humidity in the laboratory were recorded during experiment and calibration. In both cases the measured ambient temperature was 25°C, and the relative humidity was 42% (10% uncertainty), which corresponds to a mole fraction of H_2O of $1.3 \pm 0.1 \times 10^{-2}$ (Ref. 5, p. 622). The value of 1.4×10^{-2} was used because it was found to agree best with the absorption features in the measured spectra. The room-air CO_2 concentration was assumed to be 330 ppm.

The axisymmetric plasma plume produced by the torch has a maximum temperature of 3400 K at the center and was found to be close to LTE in previous work[6] under the same conditions. The

measured temperature profile was obtained from Abel-inverted profiles of the absolute intensity of the NO (1,0) rovibrational bandhead. The concentration profiles of the different species used in the simulations were then calculated by assuming chemical equilibrium at atmospheric pressure and at the measured temperatures. The measured temperature profile is plotted in Fig. 3a, and the profiles of mole fractions for the main species calculated with STANJAN are plotted in Fig. 3b. The center of the plasma corresponds to a radius value of 0. These profiles were used by the SPECAIR code to compute the absolute-intensity, line-of-sight emission spectrum.

Absolute-Intensity Calibration of the Measured Spectrum

Calibration in absolute intensity was achieved using a calibrated tungsten-ribbon lamp (Optronics Laboratories Model OL550) traceable to National Institute of Standards and Technology standards. The measured lamp spectrum is divided by the theoretical lamp spectrum to obtain the absolute response curve of the optical setup. The response curve accounts for the response of the lenses, mirrors,

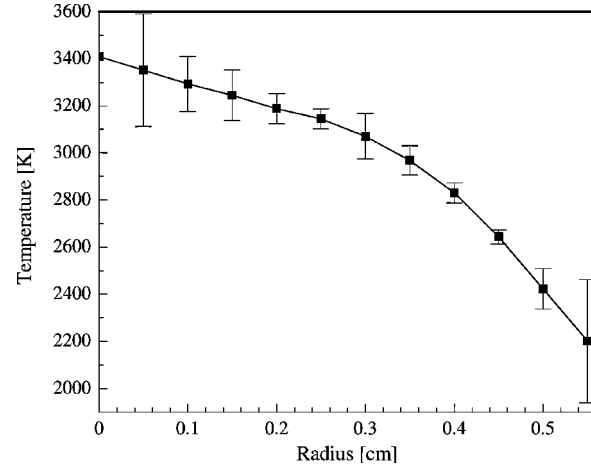

Fig. 3a Radial temperature profiles at the exit of the test section.

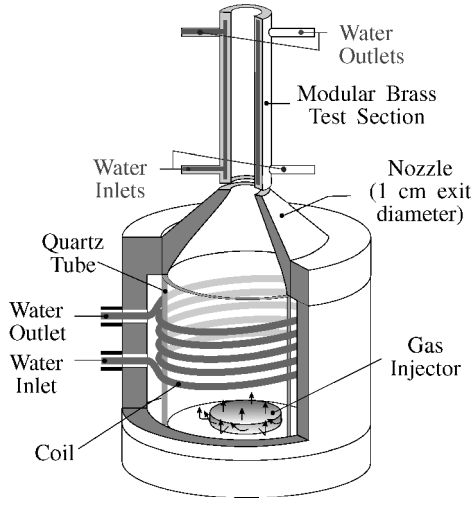

Fig. 1 Torch head and test-section schematic (not to scale).

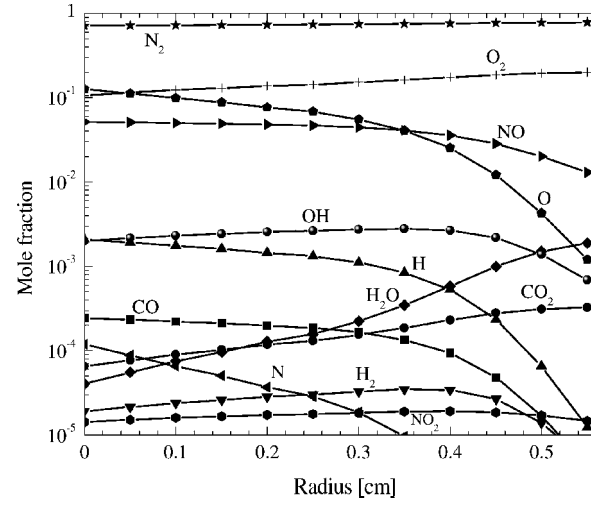

Fig. 3b Mole fraction profiles at the exit of the test section.

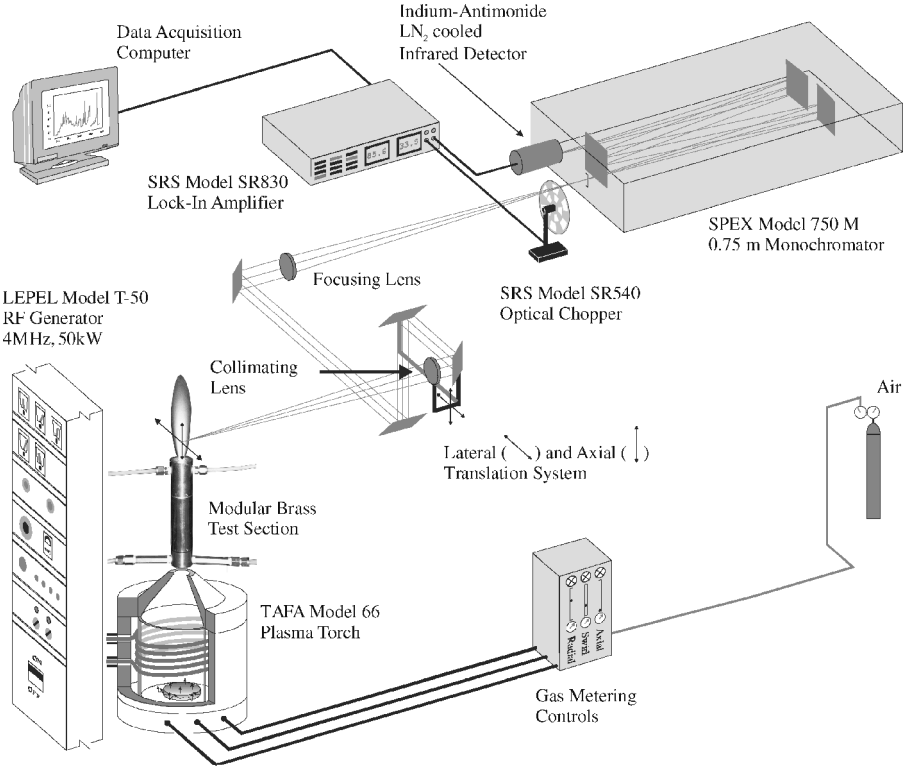

Fig. 2 Setup for optical diagnostics.

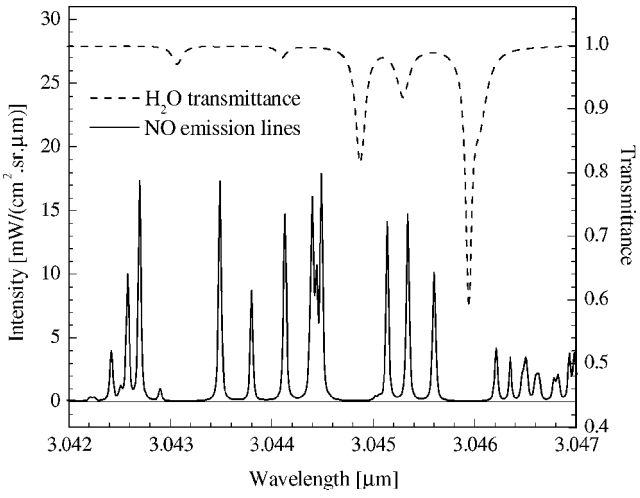

Fig. 4 NO first overtone emission lines and transmittance of 6 m of room air.

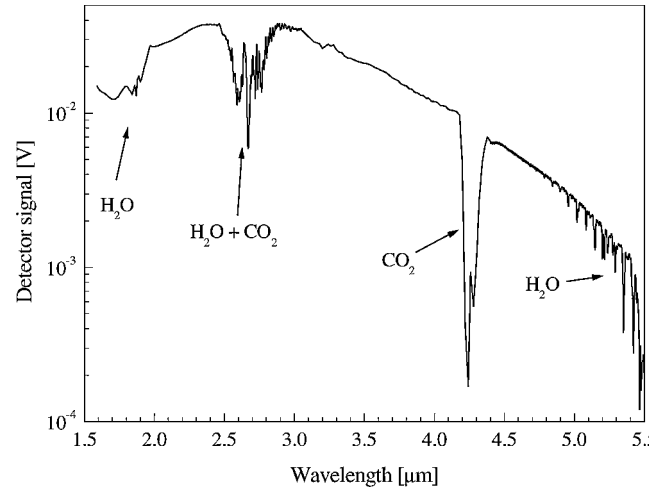

Fig. 5 Raw calibration spectrum obtained with the OL550 calibration standard.

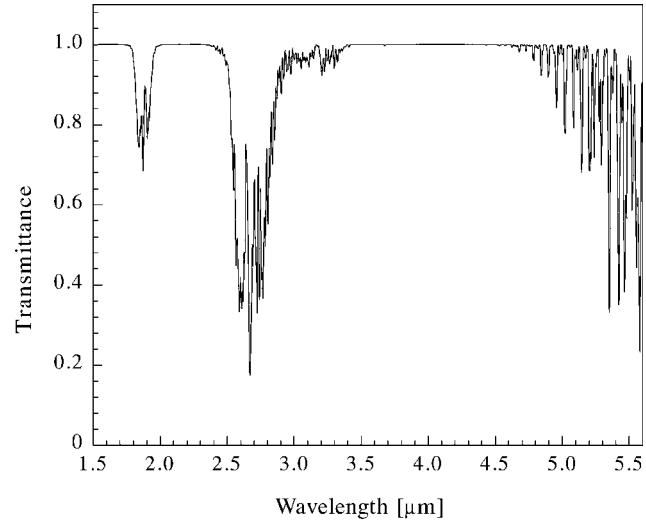

Fig. 6 Calculated H_2O contribution to the spectral transmittance of 6 m of room air.

grating and detector, and for room-air absorption. Because both the lamp spectrum and the plasma spectrum were affected by room-air absorption over the same pathlength, it could be thought possible to calibrate out the room-air absorption by simply dividing the measured raw plasma spectrum by the experimental response curve. In doing so, one would aim at canceling the absorption features in the raw plasma spectrum with those of the raw lamp spectrum. Such a procedure would be flawed, as both raw spectra are the result of the convolution of different emission spectra by the slit function of the monochromator and thus, at a given wavelength, do not generally exhibit equal levels of room-air absorption. This is illustrated in Fig. 4.

Figure 4 shows a small portion of the emission spectrum of the NO first overtone before convolution by the instrumental slit function (bottom curve), along with a plot of the spectral transmittance of 6 m of room air (top curve). The wavelength range of the plot is roughly equal to half the spectral width of the slit function of the monochromator used in the measurements; thus, only the integrated intensity over the whole range is meaningful for comparison with experimental spectra. It can be seen that in this range the integrated intensity of the NO emission is not affected by absorption. For example, the H_2O lines at 3.0449 and 3.0460 μm fall in between NO emission lines and thus absorb little plasma emission. However, the H_2O lines will significantly change the integrated intensity of the lamp spectrum in this range because the tungsten-ribbon calibration lamp exhibits a continuum-like emission. Thus, after convolution with the instrumental slit function the plasma spectrum in this range will exhibit much less absorption than the lamp spectrum.

The correct procedure to calibrate the spectrum is to first deconvolve room-air absorption from the lamp spectrum. This is relatively straightforward because the lamp emission is approximately constant over the spectral range of the slit function (~40 Å). The next step is to divide this corrected lamp spectrum by the theoretical lamp spectrum to obtain the absolute response curve of the optical setup. This response curve now accounts for the response of the lenses, mirrors, grating and detector, but not room-air absorption. The last step is to divide the raw plasma spectrum by this corrected absolute response curve. With this procedure the calibrated plasma spectrum represents the spectrum emitted by the plasma and absorbed by room air: the absorption features of water vapor and carbon dioxide remain part of the experimental emission spectrum.

To model this spectrum, we compute the spectral emission of the plasma and then solve the transport equation over a 6-m path of room air. As Fig. 4 suggests, plasma emission lines and CO_2 and H_2O absorption lines must have a position accuracy better than 1 Å in order to model the effect of room-air absorption.

Deconvolution of Room-Air Absorption Features in the Lamp Signal

The raw lamp signal (detector voltage) is shown in Fig. 5. The absorption features of room air species (CO_2 and H_2O) are indicated.

Absorption by CO_2 at 4.3 μm can be removed by a straight-line interpolation, if one assumes that the lamp spectrum without room-air absorption is smooth. This approximation is certainly valid because the tungsten-ribbon emission, the grating response, and the detector response all vary smoothly in that spectral range.

The other absorption features occur over wider wavelength ranges and cannot be deconvolved using such a simple procedure. For these features our deconvolution procedure consists in dividing the lamp spectrum by the computed spectral transmission of room-air convolved with the instrumental slit function. This procedure assumes that the lamp emission is constant at the scale of the spectral width of the slit function (~40 Å), which is reasonable. The transmission spectrum of room air was obtained with the HITRAN96 database[7] with the following parameters: room temperature of 298 K, optical path length through room air equal to 6 m, H_2O mole fraction of 1.4×10^{-2}, and CO_2 mole fraction of 330 ppm. Figures 6 and 7 show the calculated contributions of water vapor and carbon dioxide, respectively, to the transmittance of a 6-m-long room-air path.

Results of the deconvolution procedure around 1.8 and 2.7 μm are presented in Fig. 8. The thick line represents the corrected lamp spectrum using the spectral absorption coefficient determined with HITRAN. As can be seen on the figure, the deconvolution procedure at 1.8 μm produces a smoothly varying trace. At 2.7 μm the recovered spectrum still shows residual H_2O absorption lines that cannot be removed by varying the H_2O mole fraction. These residual features could be caused by inaccuracies in the HITRAN database or to

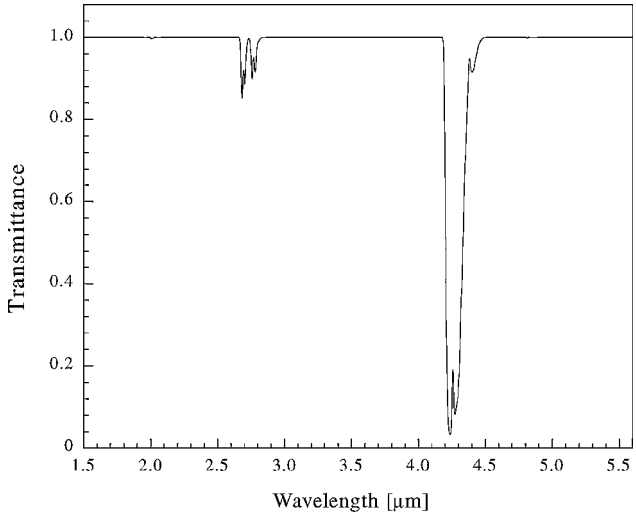

Fig. 7 Calculated CO_2 contribution to the spectral transmittance of 6 m of room air.

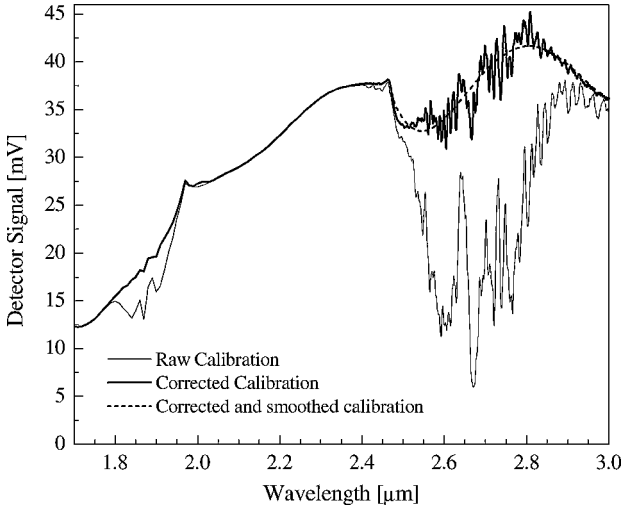

Fig. 8 Corrected calibration spectrum in range 1.7–3.0 μm. (The absorption features are caused by room-air H_2O and CO_2.)

uncertainties on the instrumental slit function. (The slit function was deduced from the entrance and exit slit widths and the theoretical dispersion of the monochromator.[2]) The corrected lamp spectrum between 2.5 and 3.0 μm shows a cusp and an S-shape variation that are likely caused by the spectral response of the ruled grating (cusps are typical in ruled-grating response curves). Because the response of the optical setup and detector should be relatively smooth, we smoothed the thick line between 2.5 and 3.0 μm with a fourth-order polynomial (dashed line).

Results of the deconvolution procedure between 4.5 and 5.5 μm are presented in Fig. 9. In this range room-air absorption is mostly due to H_2O. The small oscillations of the dashed line are caused by etalonning interference by the quartz window of the tungsten calibration lamp. These oscillations were smoothed out using adjacent averaging (thick line).

Figure 10 shows the summary comparison between the raw lamp spectrum and the corrected lamp spectrum.

The measured air plasma emission spectrum including absorption by room air, corrected for the spectral response of the detection system and calibrated in absolute intensity using the procedure discussed in the foregoing section, is presented in Fig. 11. The spectrum shows the fundamental bands of NO at ~5 μm, the ν_3 band of CO_2 at ~4.3 μm, and, superimposed between 2.5 and 4.15 μm, the lines of the OH fundamental bands, of the NO first overtone ($\Delta v = 2$) and of the ($\nu_1 + \nu_3$) band of CO_2. We summarize next our modeling of these radiative transitions.

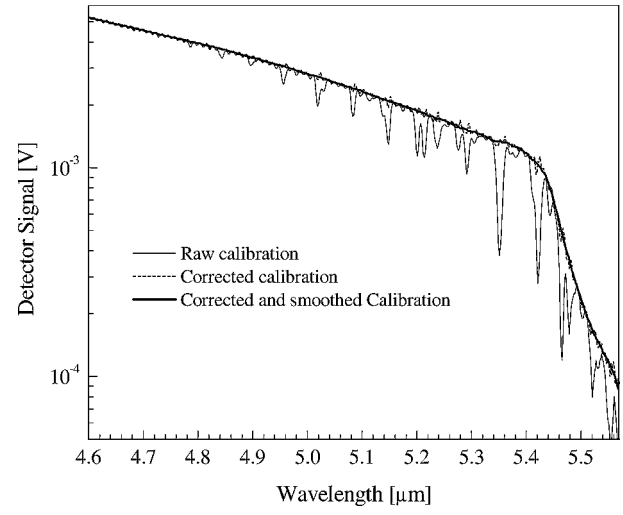

Fig. 9 Corrected calibration spectrum in range 4.6–5.6 μm. (The absorption features are caused by room-air H_2O.)

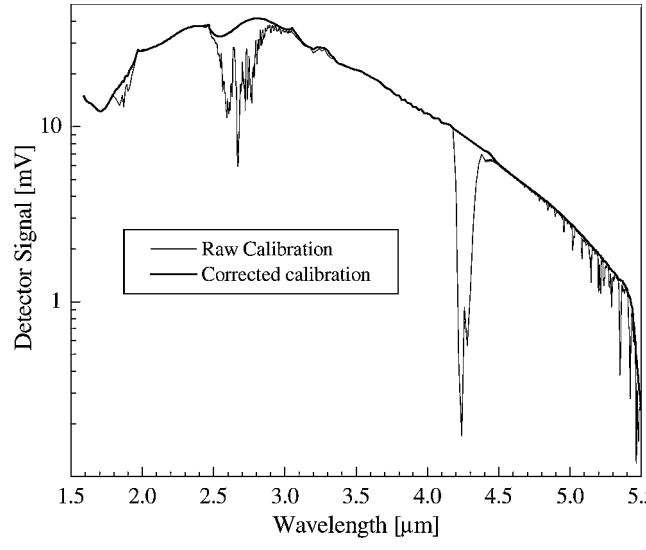

Fig. 10 Calibration spectrum corrected for water vapor and carbon-dioxide absorption.

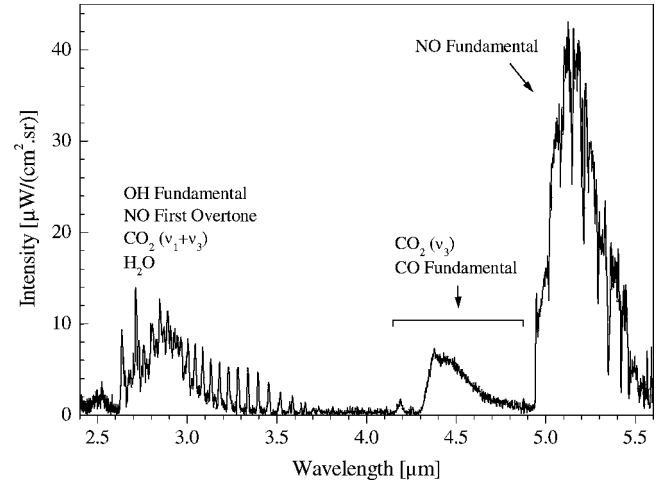

Fig. 11 Measured infrared emission spectrum for an LTE air plasma ($P = 1$ atm, maximum temperature = ~3400 K), with CO_2 and H_2O mole fractions of 3.3×10^{-4} and 2.25×10^{-3}, seen through 6 m of room air (298 K, 1 atm) with CO_2 and H_2O mole fractions of 3.3×10^{-4} and 1.4×10^{-2}.

Radiation Model

NO Rovibrational Bands

The spectroscopic model of the fundamental ($\Delta v = 1$) and overtone ($\Delta v \geq 2$) bands of NO ($X^2\Pi$) implemented in SPECAIR was previously described in Ref. 2. Rotational line positions are obtained by diagonalizing the Hamiltonian of Amiot.[8] For each vibrational band (v', v'') the vibrational dipole moments $M_{v'v''}$ are calculated as

$$(M_{v'v''})^2 = \left[\int \Psi_{v'}(r) D_e(r) \Psi_{v''}(r)\, \mathrm{d}r \right]^2$$

where D_e stands for the electric dipole moment function (EDMF), $\Psi_{v'}$ and $\Psi_{v''}$ are the vibrational wavefunctions of levels v' and v'', and r is the internuclear distance. The ab initio EDMF of Langhoff and Bauschlicher[9] is employed. Hönl–London factors (corresponding to Hund's case a) are taken from Spencer et al.[10] The model provides accurate line intensities and spectral positions, which are of particular importance for high-resolution spectroscopic diagnostics and for accurate simulation of the effect of absorption of the NO bands by atmospheric water vapor.

CO Rovibrational Bands

This system was implemented in SPECAIR using the ab initio dipole moment function of Langhoff and Bauschlicher[11] and line positions based on the spectroscopic constants of Huber and Herzberg.[12] The fundamental bands appear as a relatively weak system between 4.3 and 6 μm with a peak around 4.5 μm.

OH Rovibrational Bands

An accurate line-by-line model of fundamental and overtone bands of OH ($X^2\Pi$) was incorporated into SPECAIR. Rovibrational term energies and line positions for the 1-0 and 2-1 bands of this transition are determined by diagonalizing the Hamiltonian of Stark et al.[13] (with corrections of Levin et al.[14]). For the (3, 2), (4, 3), (2, 0), (3, 1), and (4, 2) bands we employ the term energies of Coxon.[15] As for the case of NO infrared bands, this model provides the highly accurate spectral positions required for reliable simulations of absorption by atmospheric water vapor.

Transition probabilities of the OH infrared lines are strongly affected by centrifugal distortions of the potential energy curves. As a result, the P and R branches show an anomalous distribution with intense P branches (2.6 to 4.0 μm) and very weak R branches (2.4 to 2.6 μm). In the SPECAIR model we utilize the P- and R-branch transition probabilities determined by Holtzclaw et al.[16]

CO_2 Bands at 4.3 and 2.7 μm

The temperature conditions of the present work (about 3400 K) are well above the range of applicability of the HITRAN96 database[7]; thus, the HITRAN96 database PROGCOMP could not be used. We computed the CO_2 emission spectrum with a correlated-k model[17,18] implemented by Pierrot et al.[4] The correlated-k model is a narrowband model in which the actual spectrum is replaced in each narrowband by the reordered spectrum, so that the spectral integration is carried out using typically 10 points instead of several thousands. This method is particularly well suited for the continuum-like emission of polyatomic molecules. The parameters used for the simulations presented in this paper are based on a 16-point Gaussian quadrature and a spectral decomposition over intervals of width 25 cm^{-1} and yield CO_2 radiative intensity predictions within a few percent accuracy.

Room-Air Absorption

The HITRAN96 database[7] was used to determine the transmittance spectrum of room air over a 6-m optical path. The CO_2 concentration was taken equal to 330 ppm. An H_2O mole fraction of 1.4×10^{-2} was used. First, the emission spectrum of the plasma was computed at high spectral resolution (100 points per nanometer, or approximately 10 points per linewidth), without convolution by the slit function. Then, attenuation of this spectrum as a result of water vapor and carbon-dioxide absorption was determined with Beer's law, using the line positions, line strengths, and spectral broadening coefficients of H_2O and CO_2 (HITRAN96 database). Finally, the resulting spectrum was convolved with the instrumental slit function.

Comparison of Measured and Computed Spectra

Range 4.9–5.6 μm

Figures 12 and 13 compare measurements and modeling results for the NO fundamental bands. Two simulated spectra are presented, with and without incorporating the effect of water vapor absorption over the 6-m path of room air between the plasma and the detector. By matching the depth of the water absorption features in Fig. 13, we determined the mole fraction of water vapor in the room to be approximately 1.4×10^{-2}. This value is close to the 1.3×10^{-2} mole fraction recorded during the experiment and within the uncertainties of the measurement.

As can be seen in Fig. 13, the predictions of the model (with H_2O absorption) are in excellent agreement with the measured spectrum. Because the absolute intensity of the NO (1, 0) bandhead at 4.945 μm was used for temperature determination, the calculated and experimental spectra must necessarily match at that wavelength. At longer wavelengths the emission is caused by rotational lines from higher vibrational levels. The relative intensity of these lines depends strongly on the temperature; thus, the excellent shape agreement of the spectra shows that the LTE temperature was measured

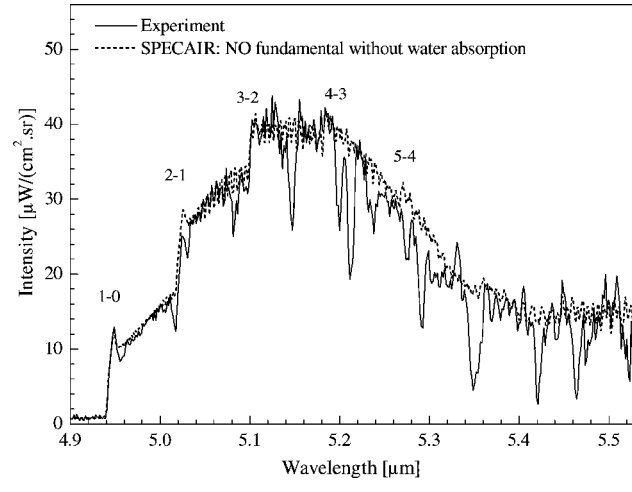

Fig. 12 NO fundamental band spectrum computed with SPECAIR without water vapor absorption and comparison with experimental spectrum. Note that a (small) constant value of 0.8 μW/(cm^2 · sr) was added to the simulated spectra to match the offset at 4.92 μm.

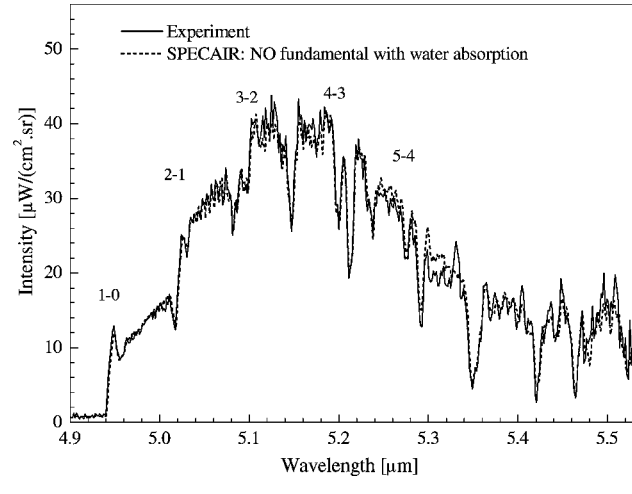

Fig. 13 NO fundamental band spectrum computed with SPECAIR with water vapor absorption and comparison with experimental spectrum.

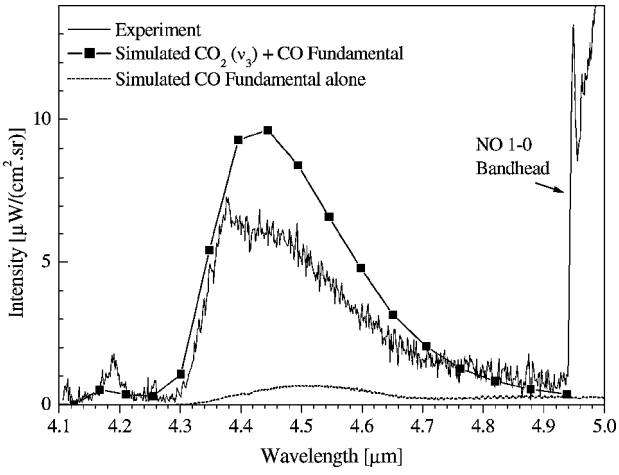

Fig. 14 Computed CO_2 spectrum (*c-k* model) and CO fundamental spectrum and comparison with the measured spectrum. Note the effects of absorption by room-air CO_2 in the range 4.2–4.4 μm.

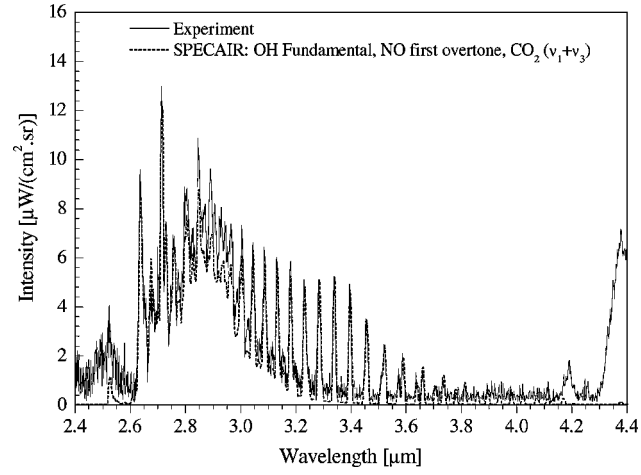

Fig. 15 Measured and modeled infrared emission spectrum of air at ~3400 K and 1 atm in the range 2.4–4.4 μm. These simulations incorporate room-air absorption.

accurately. The overall agreement validates our SPECAIR model of the NO fundamental radiation.

Range 4.1–4.9 μm

The measured CO_2 ν_3 band spectrum is compared in Fig. 14 with the predictions of the correlated-k model.[4,18] The modeled spectrum also accounts for absorption by room-air CO_2 over the 6-m optical path. This absorption is clearly responsible for near extinction in the range 4.2–4.3 μm of the emission from low-lying rotational levels of CO_2. The lines appearing beyond the edges of the absorbed region correspond to "hot" CO_2 rotational lines. The correlated-k model appears to overestimate the measured band intensity by approximately 30%. This might be because the correlated-k model is used beyond its range of applicability. (The parameters used in the model are valid only at temperatures below 2900 K.) Another possible explanation for the discrepancy might be that the air injected in the torch contained a lower concentration of CO_2 than the typical 330 ppm. However, for the simulation to agree with the measurements one would have to assume an unreasonably low CO_2 concentration of ~240 ppm. Thus we believe that the 30% intensity difference between the measured and predicted spectra is more likely caused by the use of the correlated-k model beyond its range of validity.

The rovibrational bands of CO are also modeled. As shown in Fig. 14, the fundamental bands produce a small amount of radiation in comparison with the CO_2 ν_3 and NO fundamental bands.

Range 2.4–4.2 μm

The spectrum measured in the range 2.4–4.2 μm is compared with the SPECAIR predictions in Fig. 15. As can be seen, all spectral features are well reproduced by the simulations. The contributions of NO, OH, and CO_2 are shown separately in Fig. 16.

The mole fraction of OH was determined by matching the measured absolute intensities of rotational lines of the P-branch of OH. The OH concentration determined in this manner was then used to infer the mole fraction of water in the air injected inside the plasma torch, by using chemical equilibrium relations. As already mentioned in the Introduction, the mole fraction of water injected in the torch was thus found to be approximately 2.25×10^{-3}. This value is significantly lower than the mole fraction of water vapor in room air (1.4×10^{-2}). However, the air injected in the torch was prepared by compressing atmospheric air at an earlier time when the relative humidity might have been lower. In addition, some water vapor might also have been removed by the water trap mounted at the exit of the compressed air tank.

Absorption by room air in the 6-m optical path is particularly significant between 2.5 and 2.95 μm, as can be seen in Fig. 17, where

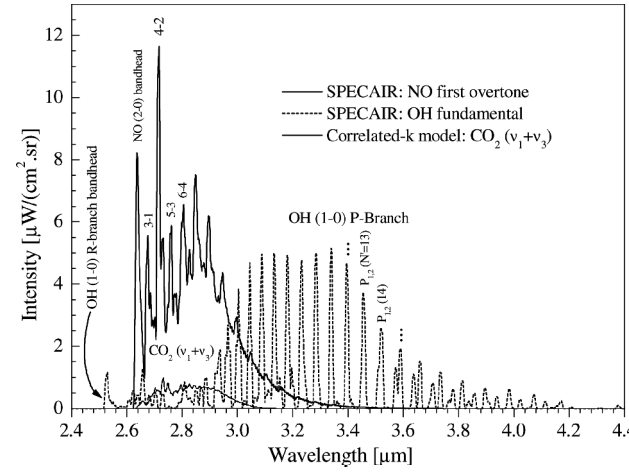

Fig. 16 Contributions of NO first overtone, OH fundamental, and CO_2 ($\nu_1 + \nu_3$) bands to the total emission spectrum in the range 2.4–4.4 μm. Note the abnormally weak OH R branch. These simulations incorporate room-air absorption.

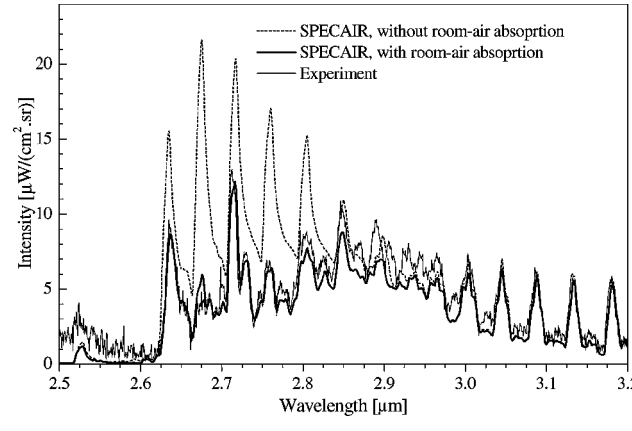

Fig. 17 Comparison between the measured emission spectrum and SPECAIR simulations with and without room-air absorption.

spectral simulations obtained with and without room-air absorption are compared with the measured spectrum. This comparison underscores the importance of computing accurate positions for all emission and absorption spectral lines, in the present case those of the NO overtone, OH fundamental, and H_2O.

Figure 18 shows the remaining difference between the experimental and calculated emission spectra including room-air absorption (solid line). The positive values indicate that some radiation is

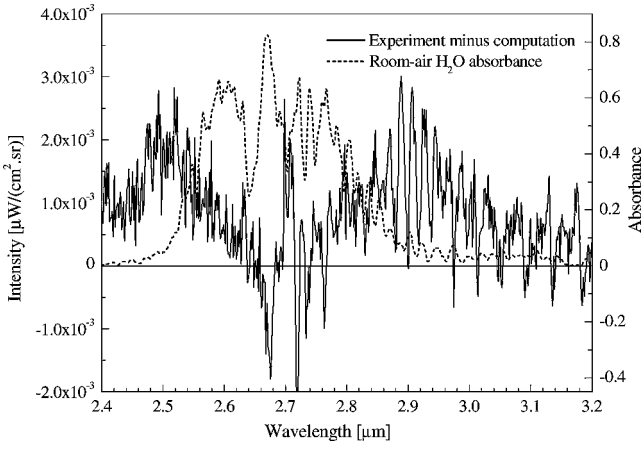

Fig. 18 Difference between experimental and computed emission spectra in the range 2.4–3.2 μm and comparison with room-air H_2O absorbance bands in this range.

missing in the emission model and seem to point to hot H_2O emission in the plasma. The room-air H_2O absorbance spectrum was superimposed in Fig. 18 to show that the missing emission is located in the spectral range of the tails of the 300 K H_2O absorbance spectrum, which suggests that hot lines of water vapor in the plasma could be responsible for the missing emission. An accurate model for H_2O emission, based on ab initio calculations, is available[19] and needs to be implemented.

Conclusions

Absolute intensity measurements and modeling of the spectral emission of an atmospheric pressure air plasma close to 3400 K were made between 2.4 and 5.5 μm. The cold gas injected in the plasma torch contained an estimated mole fraction of water vapor of $\sim 2.25 \times 10^{-3}$ and a carbon dioxide mole fraction of $\sim 3.3 \times 10^{-4}$. The main emitting systems are the fundamental and overtone bands of NO, the fundamental bands of CO, the fundamental bands of OH, and the (ν_3) and ($\nu_1 + \nu_3$) bands of CO_2. Emission by water vapor in the plasma might be present in the spectral range 2.4–3.2 μm but was not modeled. For purposes of signature detection, the most transparent region is the range 3.4–4.15 μm, in between OH rotational lines.

Special attention was paid to the effects of ambient air absorption in the optical path between the plasma and the detector. Within measurement uncertainties excellent agreement is obtained between the measured and simulated spectra of NO (absolute intensity) and OH (at least relative intensity). The correlated-k model overpredicts CO_2 emission at 3400 K by approximately 30%. Room-air CO_2 and H_2O absorption models are in excellent agreement with the experiment. Accurate models for CO_2 and H_2O emission at temperatures up to 3400 K are required to obtain better agreement between calculations and experiment over the spectral range investigated. At present there is no model available for high-temperature CO_2.

Acknowledgments

This work was supported by the Ballistic Missile Defense Organization and NASA (Grant NAG-2-1079) under the cognizance of David Mann and Winifred Huo.

References

[1]Rothman, L. S., Rinsland, C. P., Goldman, A., Massie, S. T., Edwards, D. P., Flaud, J.-M., Perrin, A., Camy-Peyrey, C., Dana, V., Mandin, J.-Y., Schroeder, J., McCann, A., Gamache, R. R., Wattsin, R. B., Yoshino, K., Chance, K. V., Juck, K. W., Brown, L. R., Nemtchechin, V., and Varanasi, P., "The HITRAN Molecular Spectroscopic Database and HAWKS (HITRAN Atmospheric Workstation): 1996 Edition," *Journal of Quantitative Spectroscopy and Radiative Transfer*, Vol. 60, No. 5, 1998, pp. 665–710.

[2]Laux, C. O., Gessman, R. J., Hilbert, B., and Kruger, C. H., "Experimental Study and Modeling of Infrared Air Plasma Radiation," AIAA Paper 95-2124, 1995.

[3]Park, C., "Nonequilibrium Air Radiation (NEQAIR) Program: User's Manual," NASA TM86707, 1985.

[4]Pierrot, L., Rivière, P., Soufiani, A., and Taine, J., "A Fictitious-Gas-Based Absorption Distribution Function Global Model for Radiative Transfer in Hot Gases," *Journal of Quantitative Spectroscopy and Radiative Transfer*, Vol. 62, July 1999, pp. 609–624.

[5]Reynolds, W. C., and Perkins, H. C., *Engineering Thermodynamics*, McGraw–Hill, New York, 1977.

[6]Gessman, R. J., Laux, C. O., and Kruger, C. H., "Experimental Study of Kinetic Mechanisms of Recombining Atmospheric Pressure Air Plasmas," AIAA Paper 97-2364, 1997.

[7]Rothman, L. S., Gamache, R. R., Tipping, R. H., Rinsland, C. P., Smith, M. A. H., Chris Benner, D., Malathy Devi, V., Flaud, J.-M., Camy-Peyret, C., Perrin, A., Goldman, A., Massie, S., Brown, L. R., and Toth, R. A., "The HITRAN Molecular Database: Editions of 1991 and 1992," *Journal of Quantitative Spectroscopy and Radiative Transfer*, Vol. 48, Nov. 1992, pp. 469–507.

[8]Amiot, C., "The Infrared Emission Spectrum of NO: Analysis of the $\Delta v = 3$ Sequence up to $v = 22$," *Journal of Molecular Spectroscopy*, Vol. 94, 1982, p. 150.

[9]Langhoff, S. R., and Bauschlicher, C. W., Jr, "Theoretical Dipole Moment for the $X^2\Pi$ State of NO," *Chemical Physics Letters*, Vol. 223, Dec. 1993, pp. 416–422.

[10]Spencer, M. N., Chackerian, C., Jr., and Giver, L. P., "The Nitric Oxide Fundamental Band: Frequency and Shape Parameters for Rovibrational Lines," *Journal of Molecular Spectroscopy*, Vol. 165, June 1994, pp. 506–524.

[11]Langhoff, S. R., and Bauschlicher, C. W., Jr., "Global Dipole Moment Function for the $X^1\Sigma^+$ Ground State of CO," *Journal of Chemical Physics*, Vol. 102, April 1995, p. 5220.

[12]Huber, K. P., and Herzberg, G., *Molecular Spectra and Molecular Structure IV. Constants of Diatomic Molecules*, Reinhold, New York, 1979.

[13]Stark, G., Brault, J. W., and Abrams, M. C., "Fourier-Transform Spectra of the $A^2\Sigma^+ - X^2\Pi\,\Delta v = 0$ Bands of OH and OD," *Journal of the Optical Society of America B*, Vol. 11, No. 1, 1994, pp. 3–32.

[14]Levin, D. A., Laux, C. O., and Kruger, C. H., "A General Model for the Spectral Radiation Calculation of OH in the Ultraviolet," *Journal of Quantitative Spectroscopy and Radiative Transfer*, Vol. 61, No. 3, 1999, pp. 377–392.

[15]Coxon, J. A., "Optimum Molecular Constants and Term Values for the $X^2\Pi\,(v \leq 5)$ and $A^2\Sigma^+(v \leq 3)$ States of OH," *Canadian Journal of Physics*, Vol. 58, 1980, pp. 933–949.

[16]Holtzclaw, K. W., Person, J. C., and Green, B. D., "Einstein Coefficients for Emission from High Rotational States of the OH ($X^2\Pi$) Radical," *Journal of Quantitative Spectroscopy and Radiative Transfer*, Vol. 49, March 1993, pp. 223–235.

[17]Pierrot, L., Soufiani, A., and Taine, J., "Accuracy of Narrow-Band and Global Models for Radiative Transfer in H_2O, CO_2, and H_2O-CO_2 Mixtures at High Temperature," *Journal of Quantitative Spectroscopy and Radiative Transfer*, Vol. 62, No. 5, March 1999, pp. 523–548.

[18]Soufiani, A., and Taine, J., "High Temperature Gas Radiative Property Parameters of Statistical Narrow-Band Models for H_2O, CO_2, and CO and Correlated-k Model for H_2O and CO_2," *International Journal of Heat and Mass Transfer*, Vol. 40, March 1997, pp. 987–991.

[19]Partridge, H., and Schwenke, D. W., "The Determination of an Accurate Isotope Dependent Potential-Energy Surface for Water from Extensive Ab-Initio Calculations and Experimental Data," *Journal of Chemical Physics*, Vol. 106, No. 11, 1997, pp. 4618–4639.